RAPID COMMUNICATIONS

PHYSICAL REVIEW B VOLUME 47, NUMBER 11 15 MARCH 1993-I

# Nonperturbative resonances in periodically driven quantum wells

Björn Birnir
*Mathematics Department, University of California at Santa Barbara, Santa Barbara, California 93106 and University of Iceland, Science Institute 3, Dunhaga, 107 Reykjavik, Iceland*

Bryan Galdrikian
*Physics Department, University of California at Santa Barbara, Santa Barbara, California 93106*

Rainer Grauer
*Mathematics Department, University of California at Santa Barbara, Santa Barbara, California 93106*

Mark Sherwin
*Physics Department, University of California at Santa Barbara, Santa Barbara, California 93106*
(Received 19 November 1992)

Energy absorption characteristics are computed for a classical and a quantum model of an infinite square well, as a function of driving amplitude and frequency. Nonperturbative resonances are observed corresponding to the replacement of states localized in phase space by more extended states. Their presence is predicted by avoided crossings in the quasienergy spectrum of the Floquet operator. The conditions under which these resonances occur can be realized in experiments on GaAs/$Al_xGa_{1-x}As$ quantum wells in intense far-infrared radiation.

In recent years, much theoretical and experimental effort has been devoted to the response of atoms to electromagnetic radiation with electric field comparable to the ionization energy $E_I$, but with photon energies $\hbar\omega \ll E_I$. The best-known experiments study the ionization of Rydberg hydrogen atoms by intense microwaves.[1] Results have been accounted for by classical and quantum models.[2]

Modern semiconductor technology has enabled the fabrication of solid-state analogues of one-dimensional atoms.[3] Using molecular-beam epitaxy, electrons in $Al_xGa_{1-x}As$ can be confined in arbitrarily-shaped "quantum wells" parallel to the direction of epitaxial growth ($z$ axis), while remaining free perpendicular to $z$. Quantum wells are typically 200–300 meV deep, with spacing $\Delta E$ between quantized subbands between several meV (well width 1000 Å) and 150 meV (well width 50 Å). For quantum wells with widths $L$ greater than a few hundred Å, it is possible (without destroying the sample) to apply oscillating electric fields with amplitude $E_0$ such that the electric-field energy $eE_0L > \Delta E$. Thus electrons in quantum wells driven by intense oscillating fields are a new system in which to study nonperturbative effects in the interaction of light with matter.

As a first step towards making predictions for experiments, we have performed classical and quantum simulations of the dynamics of a single electron in a one-dimensional square well driven by an intense oscillating electric field. The square well is a generic model for nonintegrable wells and we choose it because it is simple to fabricate. Qualitative and quantitative studies of single electrons in triangular and square quantum wells have been made by Benvenuto *et al.*[4] and Lin and Reichl.[5] These papers study the distribution and the localization of a large number of states. In distinction, we concentrate on the structure and interaction of a small number of states.

At experimentally realizable values of electric-field amplitude and frequency, we find sharp, purely quantum-mechanical energy-absorption resonances where population is efficiently transferred from the ground state to a highly excited state. The positions of these resonances are accurately predicted by avoided crossings in the quasienergy spectrum of the Floquet operator;[6] moreover we are able to completely explain them as multiphoton processes between Floquet "eigenstates."

We first present a brief discussion of the classical dynamics of a driven particle in a one-dimensional (1D) infinite square well, since many structures of the classical phase space persist in the quantum regime. The Hamiltonian is simply that of a driven particle in a 1D infinite square potential:

$$H(q,p,\tau) = p^2/2 + V_0(q) - \kappa q \sin(\tau), \tag{1}$$

where

$$V_0(q) = \begin{cases} 0, & |q| < 1 \\ \infty, & |q| \geq 1. \end{cases}$$

Note the only free parameter is $\kappa$, the unitless driving amplitude. This is perfectly general, noting the substitutions:

$$\tau \equiv \omega t, \quad q \equiv x/a, \quad \kappa \equiv F/m\omega^2 a. \tag{2}$$

Here $a$ is one-half the width of the physical well, $F$ is the magnitude of the driving force, $m$ is the effective mass,

 

and $\omega$ is the frequency of the drive. The physical position and time are $x$ and $t$, while $q$ and $\tau$ are now unitless. The appropriate unitless momentum $p$, and kinetic energy $\mathcal{E}$ are $p = P/m\omega a$, $\mathcal{E} \equiv p^2/2 = E/m\omega^2 a^2$, where $P$ and $E$ are the physical momentum and kinetic energy.

The resulting equation of motion is integrated to give

$$q(\tau) = -\kappa[\sin(\tau) - \sin(\tau_0)] + [\kappa\cos(\tau_0) + p_{\tau_0}](\tau - \tau_0) + q_{\tau_0}. \quad (3)$$

A good root finder is used to find the smallest $\tau$ such that the electron hits a wall at $q = \pm 1$. There, $p \rightarrow -p$, the next collision with the wall is found, and the process is iterated.

The classical dynamics are completely determined by the Poincaré map of the classical vector field since the Hamiltonian (1) is periodic in time. Figure 1 shows the phase space of the classical Poincaré map for $\kappa = 0.04$. The dynamics are organized by the particle's bouncing frequency $\Omega = \pi p/2$ for $\kappa = 0$ and the driving frequency $\omega = 1$. For any value of $\kappa$, the dynamics are regular at sufficiently high $p$ as the particle adjusts adiabatically to the periodic drive. The nearly horizontal trajectories at the top and bottom of Fig. 1 are invariant "Kolmogorov-Arnold-Moser" (KAM) tori. These are impenetrable by a classical particle. The oval trajectories surrounding the dominant $\Omega$:$\omega$=1:1 resonance at $p \simeq 0.62$ form the largest resonance "island." Higher-order resonances form a sequence converging toward $p = 0$. There they overlap forming a chaotic ocean as dictated by the Chirikov overlap criterion.[9] In Fig. 1, the chaotic ocean extends to a KAM surface which separates the period-three and period-one resonances.

When the last KAM surface separating the 1:3 and 1:1 resonances is destroyed, a classical particle can absorb energy by migrating from near $p = 0$ to the KAM lines above the 1:1 resonance.

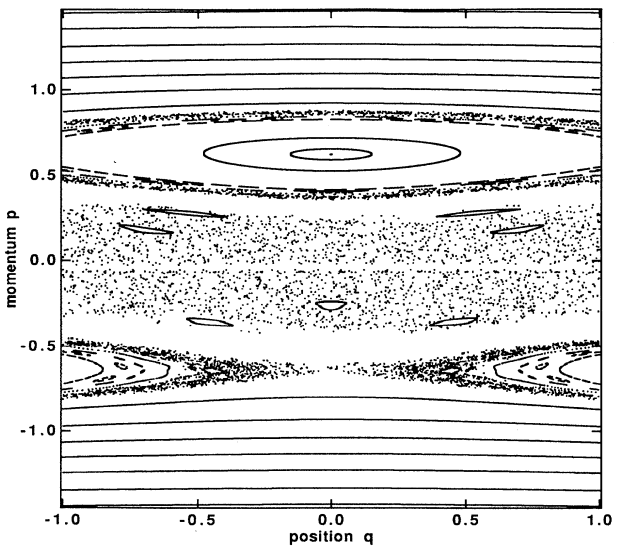


FIG. 1. The classical Poincaré section associated with the Hamiltonian [Eq. (1)], with scaled drive amplitude $\kappa = 0.04$. Trajectories are sampled at $\tau = 0 \pmod{2\pi}$.

The $(q, p)$ position of the resonances can be computed in spite of the fact that the nonlinear Poincaré map cannot be found explicitly. Moreover, the stability of the resonances can be determined because this requires only the linearized Poincaré map. This allowed us to apply Green's criterion[10,11] using the 1:$n$ resonances to estimate a value of $\kappa$ such that KAM surfaces are destroyed. This gives an estimate of $\kappa \simeq 0.05$ for the destruction of KAM surfaces between the 1:1 and 1:3 resonances.[12] We found numerically that the last KAM surface between these resonances disappears at approximately $\kappa \simeq 0.035$.

The quantum dynamics of the system are computed by solving the Schrödinger equation

$$i\hbar\partial_\tau\psi(q,\tau) = [-(\hbar^2/2)(\partial^2/\partial q^2) - q\kappa\sin(\tau)]\psi(q,\tau), \quad (4)$$

thus quantizing the Hamiltonian (1), with the boundary conditions $\psi(|q| \geq 1, \tau) = 0$. Here $\hbar$ is a *unitless* free parameter, related to the physical Planck constant by

$$\hbar = \hbar_{\text{phys}}/m\omega a^2. \quad (5)$$

Thus in addition to the purely classical parameter $\kappa$, we now have the purely quantum-mechanical parameter $\hbar$.

The temporal evolution of the state vectors is completely determined by the Poincaré map of the Schrödinger equation (4) since the latter is time periodic. But the Poincaré map is just the Floquet operator $U_{2\pi}$ (Ref. 13) which evolves a state through one drive cycle: $U_{2\pi}|\psi(0)\rangle = |\psi(2\pi)\rangle$.

We choose as a spatial basis set the energy eigenstates of the undriven well, and denote these as $\{|n\rangle\}_{n=1}^{\infty}$. In this basis, the Floquet operator can be calculated through a simple integration, using a fourth-order Runge-Kutta algorithm, evolving each basis vector through a quarter cycle of drive. The full cycle is simply calculated from the quarter cycle propagator through symmetry.

We must restrict ourselves to a finite basis for computational purposes. It suffices to choose a basis of the first $N$ states of the undriven well, where $\frac{N\pi\hbar}{2}$ is well into the KAM region in phase space. Basis states whose momentum is in the classical KAM region couple only weakly with other states. In simulating a physical system, the drive frequency determines the value of $\hbar$, from Eq. (5).

The Hamiltonian (1) is explicitly time dependent, so there are no stationary states or energy eigenvalues. Instead, since the time dependence is periodic, one computes Floquet states and quasienergies which are, respectively, the eigenfunctions and $\hbar/2\pi i$ times the Floquet exponents of $U_{2\pi}$. The analog of the classical phase portrait is the set of Husimi distributions[7] of the Floquet states. These are projections of these states onto a basis of Gaussians localized in $q$ and $p$. In such a representation the Floquet densities are seen to localize upon classical invariants, such as KAM surfaces, resonance islands, and tangles,[8] and extend themselves throughout the classically chaotic region. In this sense, a classical Poincaré section can serve as a reference to a Floquet state.

Figure 2(a) shows the energy gained by an electron with an effective mass of $\frac{1}{15}m_e$ in a 500-Å square well, as a function of field strength. Ten basis states were used. (Energy values converged to three significant digits when

five or more basis states were used.) Only the lowest two states had momenta in the classically chaotic region. The system is assumed to be in the ground state of the driven well at $\tau = 0$. After each iteration by $U_{2\pi}$, $\langle\psi|H_0|\psi\rangle$ was computed. The maximal (solid line) and mean (dashed line) over 1000 drive cycles are plotted. The Hamiltonian $H_0$ of the undriven system can be used because it is equal to the Hamiltonian of the driven system at $\tau = 0 \pmod{2\pi}$

The narrow peak in Fig. 2(a) is a purely quantum-mechanical nonperturbative resonance. In Fig. 2(a) a sharp resonance occurs as $\kappa$ (electric field) is swept through 0.78 (14.0 statvolts/cm), at a *fixed frequency* of 40 $\text{cm}^{-1}$ ($\hbar = 0.368\,275\,1$). Similar resonance peaks are found as one varies $\hbar$, or any combination of $\kappa$ and $\hbar$. (The physical drive frequency $\omega$, for example, varies both unitless parameters.)

On a resonance peak, the ground state couples to two new Floquet states that turn out to be linear combinations of Floquet states that exist off of the peak. This allows the system to gain far more energy than it would have otherwise. We say that these peaks are superimposed on the "classical" energy absorption curve, although at this highly quantum level any resemblance to the classical system is completely washed out.

We can explain these resonances as simply due to multiphoton absorption between Floquet states with different quasienergies. A view of the phase space distributions of these states on and off the peak reveals that these resonances destroy Floquet states which are localized in $p$ in favor of more extended ones. Figure 3 shows the Husimi distributions of the first and third Floquet states, just below and on the nonperturbative resonance seen in Fig. 2(a). Below the resonant value of $\kappa$ both distributions are localized in $p$. State (1,0) (the labels are defined below) is localized in the classically chaotic region of phase space and overlaps considerably with the ground state of the undriven well. State (3,4) is in the KAM region, and has virtually no overlap with the ground state. On the resonance in Fig. 2(a), the two localized states have been destroyed and replaced by two states that extend all the way from the ground-state region into the KAM region. Above the resonant value of $\kappa$, the Floquet states return to their original structure, so these states are not shown in the figure. We conclude that at the resonances, multiphoton processes allow transport from states localized in the chaotic region to states localized in the KAM region, via the extended states.

The mechanism behind the nonperturbative resonances is revealed upon examining the variation of the quasifrequency (quasienergy/$\hbar$) spectrum with relevant parameters. Each quasifrequency is associated with two indices $(n, m)$.[6] In the limit of zero driving amplitude the integer $n$ labels the eigenstates of the undriven well, $n = 1, \ldots, \infty$, and for each $n$, there exists an infinite family of quasifrequencies: $\mathcal{E}_{nm} = \mathcal{E}_{n,0} + m\hbar$. [The scaling of Eq. (2) makes the photon frequency equal to one.] Thus the quasienergies represent the combined energy of the particle in the well and the radiation field. The location of the resonances in parameter space corresponds to avoided crossings in the quasienergy spectrum.

The undriven energy eigenvalues are $\mathcal{E}_n^0 = n^2\pi^2\hbar^2/8$. This allows us to trace a Floquet state back to its origin as an energy eigenstate. For an example, in Fig. 2(b) the frequency of the third undriven eigenstate is $\mathcal{E}_3^0/\hbar = 4.089\,07$, so we assign the indices (3,4) to the Floquet

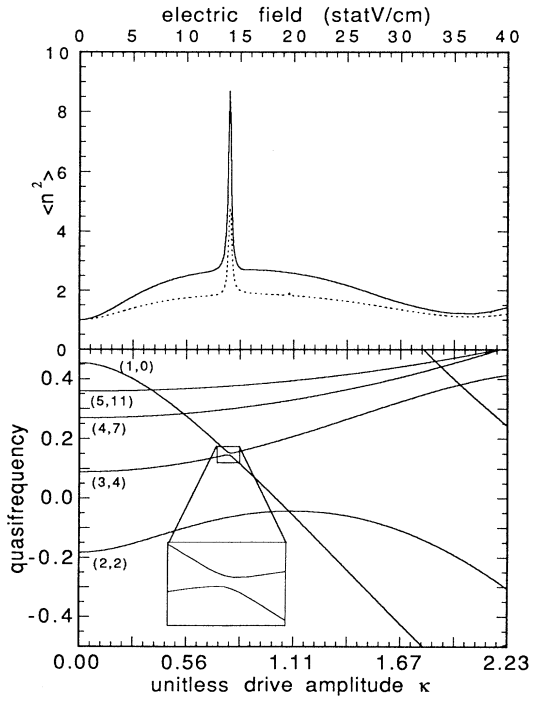


FIG. 2. (a) The maximum (solid) and mean (dashed) ensemble energy of the quantum system, varying $\kappa$. (b) Selected lines from the quasifrequency spectrum.

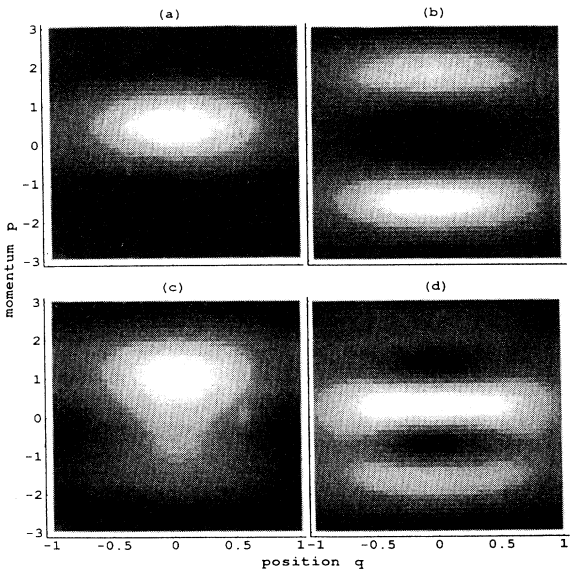


FIG. 3. The Husimi distributions of the two Floquet states which combine at the avoided crossing highlighted in Fig. 2(b). Above, (a) and (b) are the (1,0) and (3,4) Floquet states, off-resonance. Below, (c) and (d) are the more extended states formed by their combination on-resonance.

state which traces back to the quasifrequecy 0.089 07 at $\kappa = 0$. Therefore its parity[6] is $S_P = (-1)^{n+m+1} = 1$. This is the same parity as that of the Floquet state coming from the ground state, with indices (1,0). The spectral lines of two states with the same parity cannot cross, and instead avoid each other. As in standard time-independent degenerate perturbation theory, the associated eigenstates couple to form a new basis at the avoided crossing. This analysis is similar to that of Shirley,[14] in the context of two-state systems.

The 1D infinite square well with one electron is clearly a highly simplified model of electrons in a quantum well in $Al_xGa_{1-x}As$. However, neglected effects are unlikely to eliminate the existence of quasienergies, multiphoton processes at their avoided crossings, and hence the existence of nonperturbative resonances.

We cannot prove that the nonperturbative resonances persist at this stage, work in that direction is in progress, but we have the following reasons for believing that they do. For excitation energies lower than the energy of an LO phonon, such as the nonperturbative resonance in Fig. 2 which couples the ground state with the first excited state (18 meV), estimates of the time of inelastic scattering for the quantum wells range from tens to hundreds of laser cycles for the frequency used in our simulations.[15] Thus it is reasonable to ignore the finite electron coherence time as a first approximation for such resonances. The finiteness of the well is ignored, but computations modeling the continuum[16] show that the resonances are merely shifted as indicated by perturbation theory. Motion in the plane of the well is not included but can be added in a straightforward manner within the framework of dissipationless quantum mechanics. Presumably this effect is much smaller than those of many-body interactions and dissipation. We need to know what effect dissipation has on the Floquet theory of the model. Dissipation here can be treated as a composite system, coupling the electrons with a phonon bath. The work on this nontrivial task is in progress. The many-body effects need to be tackled by a time-dependent density functional theory. Such a theory does not presently exist but is being developed, see Birnir and Holthaus.[17] However, Birnir, Gudmundsson, and Johnson[18] have interlaced time iteration with Hartree iteration to compute the Poincaré map of the driven square well. These computations showed that the nonperturbative resonances persisted, but that their amplitude was modulated.

If a sufficiently low charge density is placed in a quantum well, the single-particle and many-body results must converge. We have performed self-consistent calculations of the wave functions and energy levels for an undriven, symmetrically modulation-doped 500-Å square well. For sheet densities less than $5\times10^{10}$ cm$^{-2}$, the wave functions are qualitatively unchanged by many-body effects, and the difference between energy levels shifts by less than five percent. These small changes in the static properties give one hope that the effects on quasienergies are also small for low densities.

The well widths and electromagnetic field strengths for which nonperturbative resonances were predicted in this work are achievable using $GaAs/Al_xGa_{1-x}As$ quantum wells and the free-electron laser at the University of California at Santa Barbara. Efforts are currently underway to determine the best experimental signature of these resonances, and to observe them. The most obvious experiment is to look for an increased extinction of incident radiation at a particular value of far-infrared intensity. However, it is uncertain that electrons can dissipate energy fast enough to make this effect observable. Alternatively, the average electronic kinetic energy (temperature) could be determined directly from measurements of the photoluminescence or photovoltage[20] in the presence of intense far-infrared radiation. The experimental observation of the nonperturbative resonances predicted in this work could usher in a new era in the study of nonperturbative effects in the interaction of light with matter.

We wish to thank Rainer Scharf and Bala Sundaram at Los Alamos National Laboratories for their advice. We are also grateful to Martin Holthaus, at the Center for Nonlinear Science at UCSB, for sharing his knowledge of quasienergy spectra, and to Frank Stiernelof who helped in the modeling of the quantum system. This work was supported by NSF Grants Nos. DMR 8901651 (M.S.S. and B.G.) and DMS91-04532 (B.B.), the Alfred P. Sloan Foundation (M.S.S.), and INCOR Grant No. CNLS/91-0970 (B.G.).

[1] J. Bayfield and P. Koch, Phys. Rev. Lett. **33**, 258 (1974).
[2] See, for example, G. Casati and L. Molinari, Prog. Theor. Phys. **98**, 287 (1989); R. V. Jensen *et al.*, Phys. Rep. **201**, 1 (1991).
[3] For a review, see C. Weisbuch and B. Vinter, *Quantum Semiconductor Structures* (Academic, Boston, 1991).
[4] F. Benvenuto *et al.*, Z. Phys. B **84**, 159 (1990).
[5] W. A. Lin and L. E. Reichl, Phys. Rev. A **37**, 3972 (1988).
[6] H. P. Breuer and M. Holthaus, Ann. Phys. (N.Y.) **221**, 249 (1991).
[7] S. Chang and K. Shi, Phys. Rev. A **34**, 7 (1986).
[8] E. J. Heller *et al.*, Phys. Scr. **40**, 354 (1989).
[9] B. V. Chirikov, Phys. Rep. **52**, 263 (1979).
[10] J. M. Green, J. Math. Phys. **20**, 1183 (1979).
[11] R. S. MacKay and J. D. Meiss, Phys. Rev. A **37**, 4702 (1988).
[12] B. Galdrikian, B. Birnir, and M. Sherwin (unpublished).
[13] A. H. Nayfeh and D. T. Mook, *Nonlinear Oscillations* (Wiley, New York, 1979).
[14] J. H. Shirley, Phys. Rev. **138**, 979 (1965).
[15] D. Y. Oberli *et al.*, Phys. Rev. Lett. **59**, 696 (1987).
[16] B. Galdrikian *et al.* (unpublished).
[17] B. Birnir and M. Holthaus (unpublished).
[18] B. Birnir, V. Gudmundsson, and K. Johnson (unpublished).
[19] W. Kohn and L. J. Sham, Phys. Rev. **140**, 1133 (1965).
[20] E. Batke *et al.*, Appl. Phys. Lett. **54**, 131 (1989).

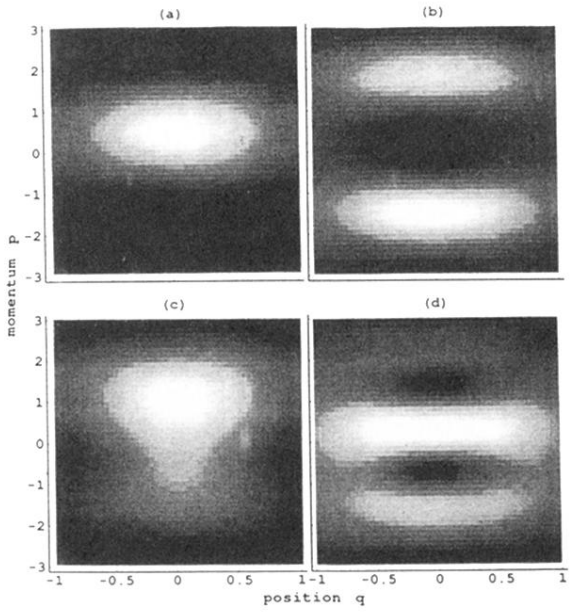


FIG. 3. The Husimi distributions of the two Floquet states which combine at the avoided crossing highlighted in Fig. 2(b). Above, (a) and (b) are the (1,0) and (3,4) Floquet states, off-resonance. Below, (c) and (d) are the more extended states formed by their combination on-resonance.